Fractal dynamics of electron wave packets in one-dimensional quasiperiodic systems

Shuji Abe
Electrotechnical Laboratory, Tsukuba Research Center, Sakura-mura, Ibaraki 305, Japan

Hisashi Hiramoto
Institute of Materials Science, University of Tsukuba, Sakura-mura, Ibaraki 305, Japan
(Received 20 February 1987)

The dynamics of an electron described by the one-dimensional tight-binding Hamiltonian with quasiperiodic (Fibonacci) modulation is studied numerically. The width of an initially localized wave packet is found to increase with time t in an overall power-law form $\sim t^{\alpha}$ $(0<\alpha<1)$. The exponent α continuously decreases with increasing strength of quasiperiodic modulation. Moreover, prominent hierarchical oscillations are found to occur in the case of strong modulation. These results are explained well by a renormalization-group argument.

Recently, numerous efforts have been devoted to understanding the electronic properties of quasiperiodic systems,[1-7] stimulated by the discovery of quasicrystals[8] and also by the fabrication of quasiperiodic superlattices.[9] A novel class of electronic states has been theoretically shown to exist in such systems: the "critical" (or intermediate) states, which are neither extended nor localized in the conventional sense.[1-5,10]

Still unknown is the implication of this new class of states on the dynamical properties of electrons or elementary excitations in general. In this paper, we study numerically the quantum-mechanical time evolution of electron wave packets in one-dimensional quasiperiodic (Fibonacci) systems where all eigenstates are known to be critical.[1-5] We will show that the wave-packet dynamics involves fractal behavior[11] in the time domain, or *fractal dynamics*: anomalous power-law diffusion and hierarchical oscillations.

We consider the one-dimensional tight-binding electron model defined by the Hamiltonian

$$H=\sum_n \varepsilon_n a_n^{\dagger}a_n+\sum_n u_{n,n+1}(a_n^{\dagger}a_{n+1}+a_{n+1}^{\dagger}a_n)\ , \qquad (1)$$

with the site (diagonal) energy ε_n and/or the nearest-neighbor transfer (off-diagonal) energy $u_{n,n+1}$ being discretely modulated according to the Fibonacci sequence. A Fibonacci modulation is written, for the off-diagonal energy, as

$$u_{n,n+1}=\begin{cases} u_a & (m-\sigma<n\sigma+\theta\leqq m) \\ u_b & (m<n\sigma+\theta\leqq m+1-\sigma)\ , \end{cases} \qquad (2)$$

where m are arbitrary integers, θ is a constant, and $\sigma\equiv(\sqrt{5}-1)/2$. We focus on this off-diagonal model in the present paper, since the results for the diagonal model turn out to be qualitatively similar. A more detailed and comparative analysis of the two models will be published elsewhere.[12]

In our numerical study, we first calculate all the eigenvalues and the eigenvectors for a given system by direct diagonalization. Then a wave packet is assumed to be initially localized on a single site $[\psi_n(t=0)=\delta_{n,n_0}]$, and its time evolution is calculated as a linear combination of that of the eigenvectors.[13] Finiteness of the system and boundary conditions is not very important for the present purpose, as long as we restrict our attention to the time region where the wave fronts do not reach the boundaries.

In the following we will show results for $|u_b/u_a|>1$. Although the present model is not symmetric with respect to the suffixes a and b, qualitatively similar results are obtained for $|u_b/u_a|<1$. Let us take, for definiteness, the Fibonacci chain with $\theta=\frac{1}{2}$ in Eq. (2) and set the initial position of a wave packet on the origin $n_0=0$, which is a center of inversion symmetry of the lattice. This renders the wave packet symmetric with respect to the origin at all times. Although this center is rather a special point of the Fibonacci lattice, this choice of the initial position does not lose the generality of the results shown below because of a reason which we will describe later.

The quantity we examine especially is the mean square displacement of the wave packet, $\langle(\Delta x)^2\rangle$, as a function of time t. Throughout the present paper we define $\Delta x\equiv n-n_0$, and we measure time in units of $1/\bar{u}$, where $\bar{u}$ is the averaged transfer energy $\bar{u}\equiv\sigma u_a+(1-\sigma)u_b$. Figure 1 shows the results of such calculations for various values of u_b/u_a. Note the logarithmic scales of the plot. Although the curves contain many oscillatory components, especially for large values of u_b/u_a, their overall behavior is described as a power law:

$$[\langle(\Delta x)^2\rangle]^{1/2}\sim t^{\alpha}\quad (t>0)\ . \qquad (3)$$

The exponent α is in the range of $0<\alpha<1$ and decreases with increasing the ratio $u_b/u_a(>1)$. In Fig. 1 we notice also that the oscillations occur in various different time and length scales in a self-similar fashion.

Examples of actual shapes of calculated wave packets during their time evolution are shown in Fig. 2. The wave packet is rather continuously extended in the case

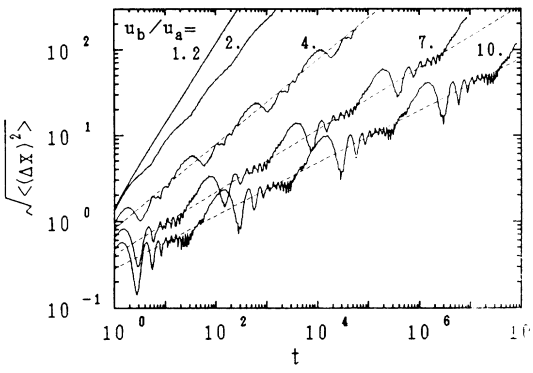

FIG. 1. Log-log plot of the length $[(\Delta x)^2]^{1/2}$ vs time t for wave packets in Fibonacci chains with $u_b/u_a = 1.2$, 2, 4, 7, and 10. The initial position of the wave packets is chosen at a center of symmetry of the Fibonacci chain. The unit length is the atomic spacing, and the unit time is the inverse of the average transfer energy $\bar{u}$.

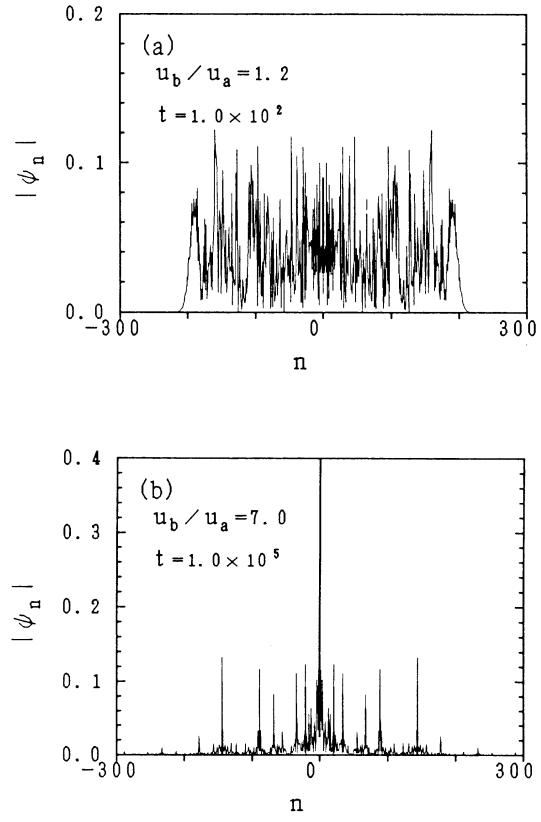

FIG. 2. Typical real-space shapes of wave-function magnitudes during their time evolutions shown in Fig. 1 for Fibonacci chains with (a) $u_b/u_a = 1.2$ and (b) $u_b/u_a = 7$. The spatial region shown here is only a portion of the whole system (2000 sites) used in the numerical experiments.

of weak modulation $|(u_b/u_a)-1| \ll 1$ [Fig. 2(a)], whereas it is rather fragmented, i.e., composed of many separate peaks, in the case of strong modulation $|u_b/u_a| \gg 1$ [Fig. 2(b)].

In Fig. 3, we plot the exponent α of Eq. (3), obtained from the results of the numerical experiments, as a function of the ratio u_b/u_a. The limit of vanishing modulation ($u_b/u_a = 1$) corresponds to $\alpha = 1$. This is because a wave packet in a periodic crystal expands continuously at a constant rate without scattering. (An initially localized wave packet is composed of all the k states in the Brillouin zone, with their group velocities spanning a limited range.) In increasing the ratio u_b/u_a, the exponent α continuously decreases, passing through the value $\alpha = \frac{1}{2}$, which corresponds to ordinary diffusion. In other words, an electron on the Fibonacci chain moves "faster" or "slower" than ordinary diffusion, depending on whether $u_b/u_a \lesssim 4$ or $\gtrsim 4$.

Let us describe dynamical behavior of wave packets in greater detail. For weak modulation, a wave packet rather continuously expands, so that its width increases smoothly, as we have seen in Fig. 1. In contrast, a wave packet in the strong modulation case is composed of separate peaks, as shown in Fig. 2(b) and, in the course of time evolution, the positions of the peaks do not vary; only their heights do. (It is found, however, that their positions depend on the initial position of the wave packet, implying that there is no *a priori* preferred position for wave packets to stay in the system.) The oscillations observed in Fig. 1 indicate that the wave-function magnitude transfers back and forth between the peaks. In fact, the peaks appear on spatial regions (clusters) whose local geometries (bond configurations) are similar to the initial region. Therefore, the oscillations are interpreted as resonance oscillations between neighboring clusters with similar local energy-level structures.

An important point is that there is *a hierarchy* of resonance oscillations with different time scales, each of

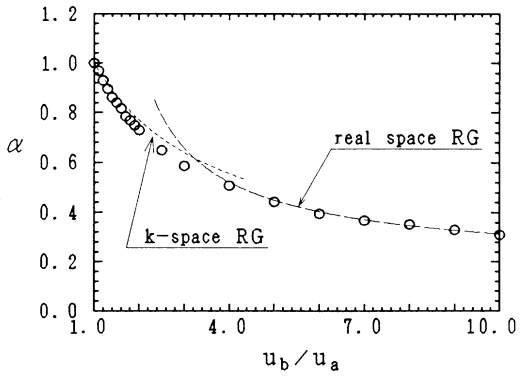

FIG. 3. Plot of the exponent α vs the ratio u_b/u_a for wave-packet dynamics in Fibonacci chains. The circles are the results of the numerical experiments. The curves are the results of the k-space and the real-space renormalization-group theories.

which corresponds to some length scale (see Fig. 1). This may be understood from the following property of the Fibonacci sequence:[14] If one takes a cluster of length l in the sequence, then one can find an exact copy of this within a distance of the same order of l. Therefore, the resonance oscillations can occur in principle in every length scale.

This interpretation of the hierarchical oscillations is further solidified by a renormalization-group (RG) approach, which in turn allows us to interpret the result of Eq. (3). In the following we give a brief description of the RG approach, a fuller discussion of which will be reported elsewhere.[12] Let us confine ourselves for the time being to the case of strong modulation, $|u_b/u_a| \gg 1$, where an approximate real-space RG scheme is constructed as follows.[6] The original Fibonacci lattice is decomposed into two sublattices: one which consists of "atoms," or single sites between two contiguous weak bonds (u_a); the other which consists of "molecules," or double sites connected by a strong bond (u_b). Then a RG transformation is defined by elimination of either of the two sublattices, which results in an effective Hamiltonian isomorphous to the original one with reduced effective transfer energies.

The main idea in applying the RG scheme to our dynamical problem is that the dynamical processes of an electron are regarded as realization of the RG procedure. That is, the complementarity relationship between time and energy implies that electron motion in a time scale t is governed by the effective Hamiltonian with the energy scale t^{-1}, which corresponds to a certain stage of the RG procedure. Let us consider the "atomic" RG procedure where one always eliminates molecular sublattices. In this case, the renormalization transformation[6] involves energy scaling by the factor $(u_a/u_b)^2$ and length scaling by the factor τ^3, where $\tau \equiv \sigma^{-1} = (\sqrt{5}+1)/2$. Then we obtain

$$\alpha \simeq \frac{3\ln\tau}{2\ln|u_b/u_a|} \quad (|u_b| \gg |u_a|) , \tag{4}$$

which corresponds to the curve indicated as "real-space RG" in Fig. 3. This should be compared with the numerical results shown in the same figure, because the initial position used in these particular numerical experiments corresponds to the site which belongs to the "atomic" sublattice at every stage of the RG procedure. Accordance between the numerical results and the real-space RG theory is satisfactory for large values of u_b/u_a.

The scaling factor for the "molecular" sites is somewhat different,[6] so that a RG procedure for a general initial position is a combination of the two RG transformations. However, it can be shown that the center of inversion symmetry ($n_0=0$) is a stable fixed point of the RG procedure. This implies that, even if one starts from a site at a finite distance from the center, one will eventually be at the center after finite RG steps. Thus the dynamical behavior of the wave packet in the limit $t \to \infty$ is determined by the fixed point. This is the reason why we have chosen the specific initial position in showing the numerical results. (Actually we have tested various initial positions in numerical experiments and observed the tendency of approach to the fixed point.)

It should be noted that the index α depends on the fixed point. There are an infinite number of fixed points, which are infinitely remote from one another, and at each of which the index α can be defined. [One can examine the properties of such fixed points by choosing different values of θ in Eq. (2).] In short, the index α has a spectrum, at least in the case of strong modulation, as a function of the global location of the initial position in the infinite Fibonacci chain. We will return to this point later.

Now let us turn to the case of weak modulation $|(u_b/u_a)-1| \ll 1$, where a RG procedure in k space may be constructed as follows.[12,7] If a small quasiperiodic modulation is treated as a perturbation to the periodic lattice, its effect is to produce energy gaps in the dispersion of the unperturbed band. Although the gaps appear at an infinite number of points densely distributed in k space, one can take into account their effects successively from the larger ones, renormalizing the band structure each time. This k-space RG scheme is applied to the wave-packet dynamics in a manner similar to the real-space RG: The dynamics of a wave packet at a time scale t is governed by the band-structure renormalized up to the order of t^{-1} in energy.

An initially localized wave packet is composed of all the k states with various group velocities, so that the rate of its expansion is determined by the mean square group velocity $\langle v^2 \rangle$. In each of the RG steps, this quantity is slightly reduced due to the flattening of the dispersion near the gaps introduced in the step. The lowest-order perturbational calculation for the RG procedure shows[12] that the time scaling by the factor τ corresponds approximately to the scaling of $\langle v^2 \rangle$ by the factor $1-(2/\pi)\delta\ln\tau$, where $\delta \equiv |(u_b-u_a)/\bar{u}|$. This yields the relationship $\langle v^2 \rangle \sim t^{-2\delta/\pi}$, which, combined with $\langle (\Delta x)^2 \rangle = \langle v^2 \rangle t^2$, leads to the power law of Eq. (3) with

$$\alpha \simeq 1-\frac{\delta}{\pi} \quad (\delta \ll 1) . \tag{5}$$

As shown in Fig. 3, this k-space RG theory is in good accordance with the numerical results in the region $|(u_b/u_a)-1| \ll 1$.

We have mentioned above that the dynamical index α has a spectrum in the case of strong modulation. It turns out that the spectrum of α in this limit corresponds exactly to that of the index α_E of the energy spectrum obtained by Kohmoto, Sutherland, and Tang.[4] (Note that the former is a spectrum with respect to spatial position and the latter, with respect to energy.) However, this correspondence does not hold in the case of weak modulation. This is obvious from the fact that in the case of vanishing modulation the dynamical index α should be simply 1 (i.e., coherent motion), whereas the spectrum index α_E is 1 at the band center and $\frac{1}{2}$ at the band edges. For small δ, the index α is approximately given by Eq. (5) within the order of δ and may have a

spectrum with a small width of a higher order in δ. The reason why the spectrum of our dynamical index α shrinks in the weak modulation limit is that it originates from the site dependence of Green's function, which becomes less significant for smaller modulations. The exact dependence of the dynamical index α (and its spectrum) on the modulation strength in the whole region and its relation to static indexes, such as α_E, are open questions at present.

Fractal dynamics shown in the present paper is likely to be a universal feature of the critical states in many quasiperiodic systems, including quasicrystals in higher dimensions.[14] Note that it is not a property of a single eigenstate, but rather that of a collection of eigenstates over a certain energy range. Therefore, it may have some connection to the electrical conductance at finite temperatures or at finite frequencies. Direct experimental observation of the wave-packet dynamics will be possible in semiconductor Fibonacci superlattices[9] by detecting propagation of various elementary excitations. Also promising is optical transition from some impurity state to band states, which provides a localized initial wave packet just after photon absorption.

In conclusion, we have shown by the numerical experiments that electron motion in the Fibonacci chain is characterized by fractal dynamics, i.e., anomalous diffusion and hierarchial oscillations. The renormalization-group argument gives a natural explanation of the results.

We thank Dr. J. Kondo for stimulating discussions.

[1]M. Kohmoto, L. P. Kadanoff, and C. Tang, Phys. Rev. Lett. **50**, 1870 (1983).
[2]S. Ostlund, R. Pandit, D. Rand, H. J. Schellnhuber, and E. D. Siggia, Phys. Rev. Lett. **50**, 1873 (1983).
[3]M. Kohmoto and J. R. Banavar, Phys. Rev. B **34**, 563 (1986).
[4]M. Kohmoto, B. Sutherland, and C. Tang, Phys. Rev. B **35**, 1020 (1987).
[5]K. Machida and M. Fujita, Phys. Rev. B **34**, 7367 (1986).
[6]Q. Niu and F. Nori, Phys. Rev. Lett. **57**, 2057 (1986).
[7]T. Ninomiya, J. Phys. Soc. Jpn. **55**, 3709 (1986).
[8]D. Shechtman, I. Blech, D. Gratias, and J. W. Cahn, Phys. Rev. Lett. **53**, 1951 (1984).
[9]R. Merlin, K. Bajema, R. Clarke, F.-Y. Juang, and P. K. Bhattacharya, Phys. Rev. Lett. **55**, 1768 (1985).
[10]J. B. Sokoloff, Phys. Rep. **126**, 189 (1985).
[11]B. B. Mandelbrot, *The Fractal Geometry of Nature* (Freeman, New York, 1977); also see Proceedings of a Symposium on Fractals in the Physical Sciences, edited by M. F. Shlesinger, B. B. Mandelbrot, and R. J. Rubin [J. Stat. Phys. **36**, (5/6) (1984)]
[12]H. Hiramoto and S. Abe (unpublished).
[13]The initial condition of the δ-function form implies that we are actually calculating the time dependence of the Green function. Time evolution of a wave packet for arbitrary initial conditions can be calculated from this Green function.
[14]D. Levine and P. J. Steinhardt, Phys. Rev. B **34**, 596 (1986); J. E. S. Socolar and P. J. Steinhardt, Phys. Rev. B **34**, 617 (1986).